PREDICTION OF FAILURE PRESSURE AND LEAK RATE OF STRESS CORROSION CRACKS*

by

S. Majumdar, K. Kasza, J. Y. Park, and S. Bakhtiari
Energy Technology Division
Argonne National Laboratory
Argonne, IL 60439 USA

Phone: 630-252-5136 Fax: 630-252-4798 Email: majumdar@anl.gov

January 2002

Manuscript submitted for presentation at the 4th CNS International Steam Generator Conference, May 5-8, 2002, Toronto.

*Work supported by the U.S. Nuclear Regulatory Commission, under NRC Job Code W6487.

PREDICTION OF FAILURE PRESSURE AND LEAK RATE OF STRESS CORROSION CRACKS*

S. Majumdar, K. Kasza, J. Y. Park, and S. Bakhtiari

ABSTRACT

An "equivalent rectangular crack" approach was employed to predict rupture pressures and leak rates through laboratory generated stress corrosion cracks and steam generator tubes removed from the McGuire Nuclear Station. Specimen flaws were sized by post-test fractography in addition to a pre-test advanced eddy current technique. The predicted and observed test data on rupture and leak rate are compared. In general, the test failure pressures and leak rates are closer to those predicted on the basis of fractography than on nondestructive evaluation (NDE). However, the predictions based on NDE results are encouraging, particularly because they have the potential to determine a more detailed geometry of ligamented cracks, from which failure pressure and leak rate can be more accurately predicted. One test specimen displayed a time-dependent increase of leak rate under constant pressure.

Energy Technology Division, Argonne National Laboratory, Argonne, IL 60439

Phone: 630-252-5136 Fax: 630-252-4798 Email: majumdar@anl.gov

*Work supported by the U.S. Nuclear Regulatory Commission, under NRC Job Code W6487.

PREDICTION OF FAILURE PRESSURE AND LEAK RATE OF STRESS CORROSION CRACKS*

S. Majumdar, K. Kasza, J. Y. Park, and S. Bakhtiari

INTRODUCTION

For typical unflawed steam generator (SG) tubes made of Alloy 600, the burst pressure, p_b, at room temperature is ≈ 9.4 ksi (65 MPa). However, operating experience with pressurized water reactor (PWR) SGs in both the U.S. and abroad has shown that cracks of various morphologies can and do occur in steam generator tubes, starting early in life. These may be single cracks that are axial or circumferential, inside or outside diameter (ID or OD) initiated, and part or complete throughwall; they may also be multiple cracks that are parallel or form a network. Tests have shown that, depending on the location and morphology of these cracks, the tubes can be weakened relative to unflawed tubes to various extents.

Stress corrosion cracks (SCCs) are generally nonplanar, ligamented, and much tighter than machined flaws. They can also have highly complex geometry. Such cracks can be detected and sized using advanced eddy current (EC) nondestructive evaluation (NDE) techniques. Detection of cracks and assessment of the leak rate and structural integrity of cracked SG tubing during normal operation and accident conditions are of interest because failure of the tubes, including those that have been repaired (e.g., by sleeving), could lead to bypass of the containment. The challenge is to develop a procedure for predicting ligament rupture and leak rate for such complex cracks from the NDE signals.

Several correlations are available for predicting ligament rupture pressure of axial and circumferential, part-throughwall rectangular cracks under normal operation, design-basis accident, and severe accident conditions.[1-4] We can currently predict failure pressures and leak rates of tubes with machined flaws that are rectangular.[5] However, such a morphology is not characteristic of the SCCs observed in SGs. It is not clear as to how much detail is needed on the complex morphology of the cracks before the structural integrity of the tubes can be assessed by mechanistic models. To address this issue, the Nuclear Regulatory Commission (NRC) is sponsoring a multi-year research effort at Argonne National Laboratory (ANL). Tasks include the following: (1) produce SCC degraded tubes in the laboratory, (2) characterize by NDE the flaws in these specimens and SG tubes removed from the McGuire Nuclear Station, (3) conduct tests on these specimens in the Pressure and Leak Rate Testing Facilities at ANL at 282°C and room temperature, and (4) develop and validate correlation models for leak rate and rupture. In this paper, we evaluate a new method for investigating complex-shaped cracks, based on the

*Work supported by the U.S. Nuclear Regulatory Commission, under NRC Job Code W6487.

concept of an equivalent rectangular crack that can be determined from fractography or EC/NDE data. Failure pressures and leak rates predicted by this method are compared with results frompreliminary tests conducted to date.

FAILURE MODELS

The critical pressures and crack sizes for the unstable failure (rupture) of a thin-wall, internally pressurized, cylindrical shell with a single throughwall axial crack can be estimated with an equation originally proposed by Hahn[6] and later modified by Erdogan[7]:

$$p_{cr} = \frac{\bar{\sigma} h}{mR} = \frac{p_b}{m}, \tag{1a}$$

where:

$$\bar{\sigma} = \text{ flow stress } = k(S_y + S_u)(\text{with } k = 0.5\text{-}0.6), \tag{1b}$$

S_y and S_u = yield and ultimate tensile strengths, respectively, (1c)

$$m = 0.614 + 0.481\lambda + 0.386\exp(-1.25\lambda), \tag{1d}$$

$$\lambda = \left[12(1-\nu^2)\right]^{\frac{1}{4}} \frac{c}{\sqrt{Rh}} = \frac{1.82c}{\sqrt{Rh}}, \tag{1e}$$

$$p_b = \frac{\bar{\sigma} h}{R} = \text{burst pressure of an unflawed virgin tubing}, \tag{1f}$$

R and h = mean radius and wall thickness of tube, respectively, (1g)

ν = Poisson's ratio, and (1h)

2c = axial crack length. (1i)

A general failure criterion for predicting rupture of the crack tip ligament in a tube with a part-throughwall crack can be expressed as follows:

$$\sigma_{lig} = \bar{\sigma}, \tag{2a}$$

where σ_{lig} is the average ligament stress, which for the axial crack is given by

$$\sigma_{lig} = m_p \sigma\ , \tag{2b}$$

where m_p is the ligament stress magnification factor (which depends on the axial crack length and depth), and σ is the nominal hoop stress (calculated using the mean radius and thickness of the tube, including the sleeve, if any).

Various expressions are available for m_p of rectangular, part-throughwall axial cracks.[1-4] For this paper, we adopt the ANL correlation described in Ref. 4 and reproduced below, because it provides the best correlation for the failure pressures of the tests conducted at Pacific Northwest National Laboratory on flawed SG tubes.[3,4] This correlation is

$$m_p = \frac{1 - \alpha \dfrac{a}{mh}}{1 - \dfrac{a}{h}} \tag{3a}$$

$$\alpha = 1 + \beta \left(\frac{a}{h}\right)^2 \left(1 - \frac{1}{m}\right), \tag{3b}$$

where a is crack depth and β=1.

Equivalent Rectangular Crack*

A typical crack depth profile of an SCC is shown in Fig. 1a. No widely accepted models are available for predicting the ligament failure pressure of such SCCs. From a limit analysis viewpoint, it can be argued that the collapse behavior of a crack tip ligament with an irregular point-by-point variation of crack depth should be similar to that of a crack with a smoothed-out, "average" crack-depth profile. Local variations in crack depth and geometry are smoothed out in the EC measurements because the EC signals are averaged over a finite volume, and hence, the EC data tend to show a relatively smooth variation of crack depth along the crack length (for example, Fig. 1a). For the present, we assume that the average profile measured by the dvanced EC/NDE method is the one that is relevant for limit analysis. From the viewpoint of this assumption and plastic collapse of the ligament, the tube profile has a smoothly varying average ligament thickness (or crack depth), although the real crack may have short throughwall segments at a number of locations (deep SCCs sometimes leak when pressurized with 0.3 MPa air, but do not have measurable water leak rates until much higher pressures).

The equivalent rectangular crack is determined from the measured crack depth profile by considering all possible candidate crack lengths (≤ full crack length, an example is shown in Fig. 1b), determining the equivalent depths by equating areas (e.g., the hatched areas in Fig. 1b) so

---

* Similar equivalent rectangular crack approaches have been used by others, e.g., see report by Aptech Engineering Services, Inc., in Docket No. 50-361, "Steam Generator Run Time Analysis for Cycle 9, San Onofre Nuclear Generating Station, Unit 2, September 25, 1997."

that the actual areas of the cracks are equal to the areas of the candidate equivalent rectangular cracks, and selecting the crack having the highest m_p (i.e., lowest ligament rupture pressure). For leakage calculations, the throughwall crack length after ligament rupture is assumed to equal the length of the equivalent rectangular crack.

LEAK RATE MODEL

The formula used to calculate the volumetric leak rate Q is the standard orifice discharge equation:

$$Q = 0.6A\sqrt{\frac{2\Delta p}{\rho}} \tag{4}$$

where A is the flaw opening area, Δp is the pressure differential across the tube wall, and ρ is the density.

For the axial crack opening area, we use the Zahoor model[8] for an axial throughwall crack in a thin-walled tube:

$$A = 2\pi c_e^2 V_o \sigma / E, \tag{5}$$

where

σ = hoop stress = $\Delta pR/h$,

E = Young's modulus,

$$V_o = 1 + 0.64935\lambda_e^2 - 8.9683\text{x}10^{-3}\lambda_e^4 + 1.33873\text{x}10^{-4}\lambda_e^6,$$

$$\lambda_e^2 = c_e^2 / Rh,$$

$$c_e = c\left[1 + \frac{F}{2}\left(\frac{\sigma}{S_y}\right)^2\right],$$

$$F = 1 + 1.2987\lambda^2 - 2.6905\text{x}10^{-2}\lambda^4 + 5.3549\text{x}10^{-4}\lambda^6, \text{ and}$$

$$\lambda^2 = c^2 / Rh.$$

Both the ligament rupture pressure and leak rate equations have been validated with tests on rectangular machined notches at ANL.[5] Examples are shown in Figs. 2a and 2b.

TEST METHOD

Leak and rupture tests were conducted on two types of laboratory-generated SCC specimens and specimens from a retired McGuire SG. To facilitate the initiation and growth of SCCs in the laboratory, the first set of specimens was subjected to a high-temperature treatment that reduced the flow stress by about 20%. The second set of specimens did not have the high-temperature treatment, and their flow stress was virtually unchanged as compared to as-received material. The specimens from the McGuire Nuclear Station were tested in the as-received condition.

RESULTS

Heat-Treated Laboratory Specimens

Figure 3a shows the crack depth profiles of specimen SGL 480 measured by pre-test NDE and post-test fractography. The predicted ligament rupture pressures corresponding to the NDE and fractography profiles are 9.2 and 8.9 Mpa,. respectively, compared to the experimentally measured pressure of 6.2 MPa at onset of first leakage. At the final test pressure of 15.1 MPa, the throughwall crack length is predicted to be 10.7 and 12.7 mm by the NDE and fractography profile, respectively. The measured leak rates (Fig. 3b) follow the predicted curve reasonably closely. The post-test OD view of the crack (Fig. 4) shows the open portion to be ≈ 12.7 mm. Both the final crack length and the final leak rate are closer to the predictions based on fractography than NDE.

The crack depth profiles of specimen SGL 494 measured by pre-test NDE and post-test fractography are shown in Fig. 5a. The ligament rupture pressures corresponding to the NDE profile and fractography profile are 33.1 and 35.9 MPa, respectively. Both profiles predict the crack to become unstable after some crack growth. The leak rates are also predicted to increase rapidly immediately after ligament rupture (Fig. 5b). The test showed the leak rate to increase from zero to almost 47.3 L/min abruptly at a pressure of 32-33 MPa. The post-test OD view of the crack (Fig. 6) shows that itsopen portion is much larger compared to that of SGL 480 (Fig. 4), and the evidence of tearing at the crack tip suggests that this specimen was close to burst, as predicted.

Predictions for leak rate are not as accurate for tests SGL-493 and SGL-413 (Figs. 7a-b), which started to leak much earlier than predicted. However, with increasing pressure the measured leak rate curves tend to converge to the predicted leak rate curves based on the fractography data on depth. In most cases, the measured leak rates are closer to the predictions based on fractography than the NDE data.

As-received Laboratory Specimens

Figure 8a shows the depth profiles as measured by EC/NDE and fractography for an as-received specimen (later used in test SGL-731). Figure 8b compares the predicted and experimental pressure vs. leak rates for test SGL-731, which was conducted at room temperature. Similar comparisons for a high-temperature test, SGL-822, are shown in Figs. 9a and 9b. Both fractography and EC/NDE results indicated significant throughwall penetration of the crack for SGL-731. As a result, the leak rates are predicted to start at very low pressures. In contrast, test SGL-822 showed no measurable leakage before 14 MPa (2 ksi) pressure. During a 30-min hold at 17 MPa (2.5 ksi), the leak rate in this specimen increased from 6 to 18 L/min (1.6 to 4.8 gpm). Currently, we do not have the ability to predict such time-dependent increase of leak rate at constant pressure.

McGuire Tubes

Six McGuire tubes [19-mm (0.75-in.) dia alloy 600] were inspected by EC/NDE prior to pressure and leak rate testing at room temperature, and the depth profiles of cracks in four tubes were determined by post-test fractography. Flow stress data of the McGuire tubes tested were obtained from the mill certificates.* Observed vs. predicted rupture pressures are plotted in Fig. 10a. Most of the SCCs were shallow and, consequently, did not rupture during the tests, in agreement with predictions using the higher flow stress. The only exception was test 39-57-2, which experienced ligament rupture at 36 MPa (5.16 ksi) and was predicted to fail at 61 MPa (8.9 ksi) based on the EC/NDE profile. The depth profile for the flaw in this specimen will be determined by fractography in the future. The observed leak rates for test 4-43-2 are compared with predicted leak rates in Fig. 10b. Both the test data and the predictions show a rapid increase of leak rate with pressure immediately after ligament rupture. The comparisons in Figs. 10a-b suggest that the observed results are consistent with predictions.

DISCUSSION AND CONCLUSIONS

A procedure based on defining an equivalent rectangular crack was used to predict the ligament rupture pressure, throughwall crack length extension, and leak rate in specimens containing SCCs. The predictions were based on crack depth profiles measured by post-test fractography and pre-test EC/NDE. In two heat-treated specimens, ligament rupture pressures and leak rates were quite close to predicted values, while in two others leakage started at much lower pressures than predicted, although the measured leak rates approached the predicted leak rates at higher pressures. In two as-received specimens with relatively deep SCCs, leakage started at slightly higher pressures than predicted. One of these specimens displayed a time-dependent increase of

---

* Private Communication, R. Keating, Westinghouse Electric Company, to S. Majumdar, Argonne National Laboratory, January 25, 2002.

leak rate during a constant pressure hold at 282°C. Such time-dependent behavior at this temperature is not predicted by any available model. In most cases, test data were closer to the predictions made on the basis of crack depth profiles measured by fractography rather than EC/NDE. Nonetheless, the predictions based on EC/NDE are encouraging, and efforts to improve the sizing accuracy by advanced signal processing of the EC/NDE data are continuing at ANL. A limited number of leak and rupture tests were conducted at room temperature on six specimens from the McGuire Nuclear Station. Except for a single test, the test results are in reasonable agreement with predictions.

REFERENCES

1. J. F. Kiefner, W. A. Maxey, R. J. Eiber, and A. R. Duffy, "Failure stress levels of flaws in pressurized cylinders," in Progress in Flaw Growth and Fracture Toughness Testing, Kaufman, J. G., ed., National Symposium on Fracture Mechanics, American Society for Testing and Materials, Committee E–24 on Fracture Testing of Metals, ASTM Special Technical Publication 536, Philadelphia, 1973.

2. B. Flesch and B. Cochet, "Crack stability criteria in steam generator tubes," Int. Cong. on Pressure Vessel Technology, Beijing, Sept. 1988.

3. J. M. Alzheimer, R. A. Clark, C. J. Morris, and M. Vagins, "Steam generator tube integrity program phase I report," NUREG/CR–0718, PNL-2937, Richland, WA, Sept., 1979.

4. S. Majumdar, W. J. Shack, D.R. Diercks, K. Mruk, J. Franklin, and L. Knoblich, "Failure behavior of internally pressurized flawed and unflawed steam generator tubing at high temperatures – experiments and comparison with model predictions," NUREG/CR–6575, ANL–97/17, Argonne, IL, 1998.

5. S. Majumdar, K. Kasza, and J. Franklin, "Pressure and leak-rate tests and models for predicting failure of flawed steam generator tubes," NUREG/CR-6664, ANL-99/23, Argonne National Laboratory, Argonne IL 2000.

6. G. T. Hahn, M. Sarrate, and A. R. Rosenfield, "Criteria for crack extension in cylindrical pressure vessels," Int. J. Fracture Mech. Vol. 5, No. 3, pp. 187–210, 1969.

7. F. Erdogan, "Ductile failure theories for pressurized pipes and containers," Int. J. of Pres. Ves. & Piping, Vol. 4, pp. 253–283, 1976.

8. A. Zahoor, Ductile Fracture Handbook, Electric Power Research Institute, Palo Alto, CA, 1989.

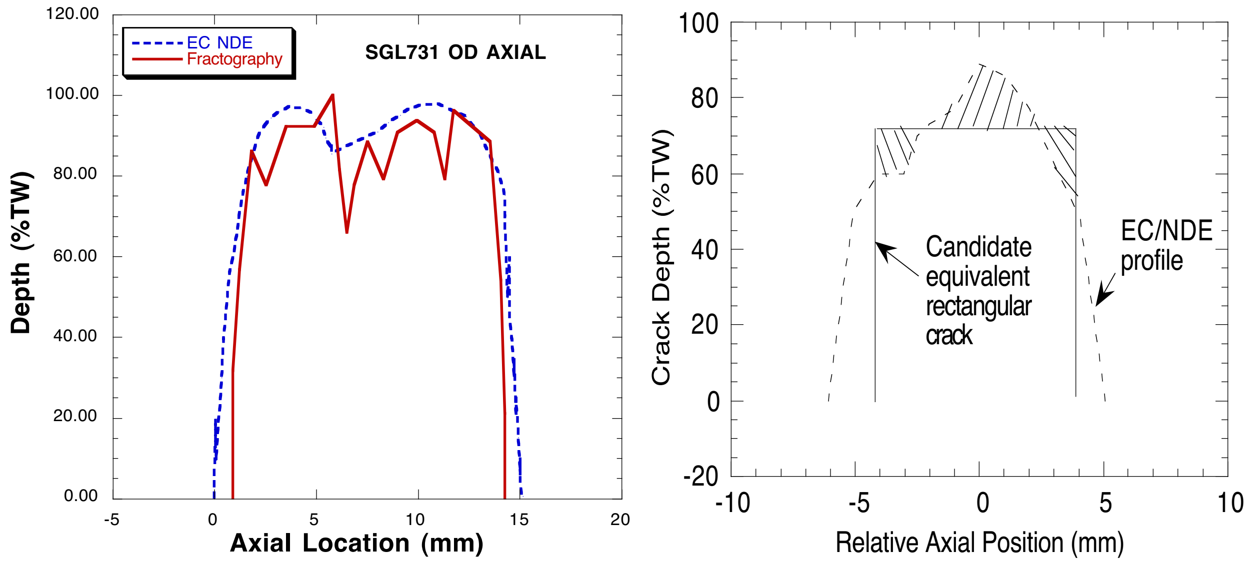

(a) (b)

Fig. 1. (a) Crack depth profile in specimen SGL-731 as measured by EC/NDE and fractography and (b) a typical candidate equivalent rectangular crack.

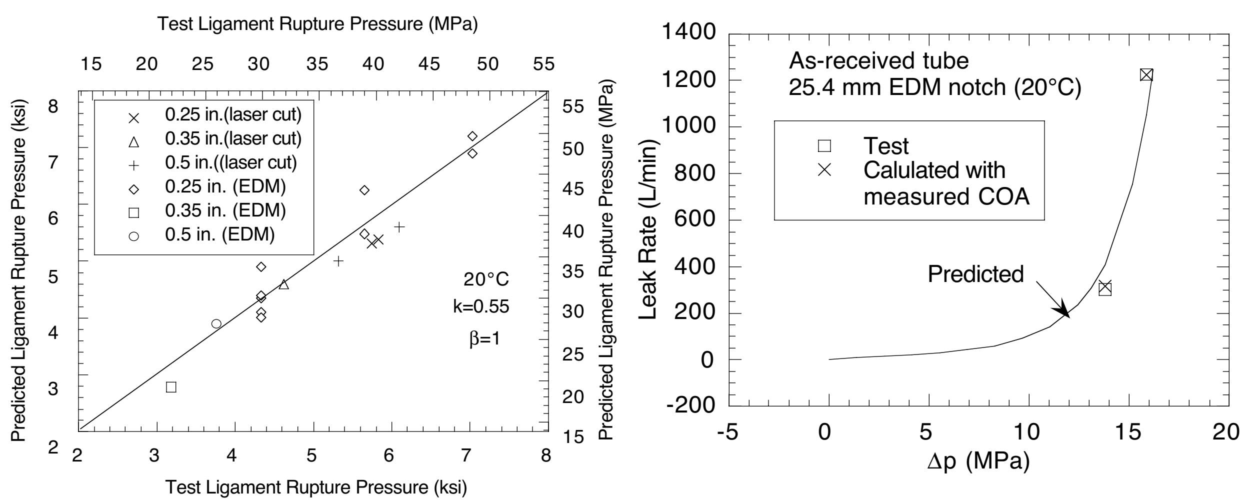

(a) (b)

Fig. 2. (a) Predicted vs. observed ligament rupture pressures for rectangular electrodischarge machined (EDM) and laser cut flaws and (b) calculated (solid line) vs. experimentally measured (symbols) leak rates for 22-mm (7/8 in.)-diameter tube with 25.4-mm (1 in.) throughwall axial EDM notches. Cross symbols (x) in Fig. 2b denote calculated leak rates using posttest measured crack opening areas (COAs).

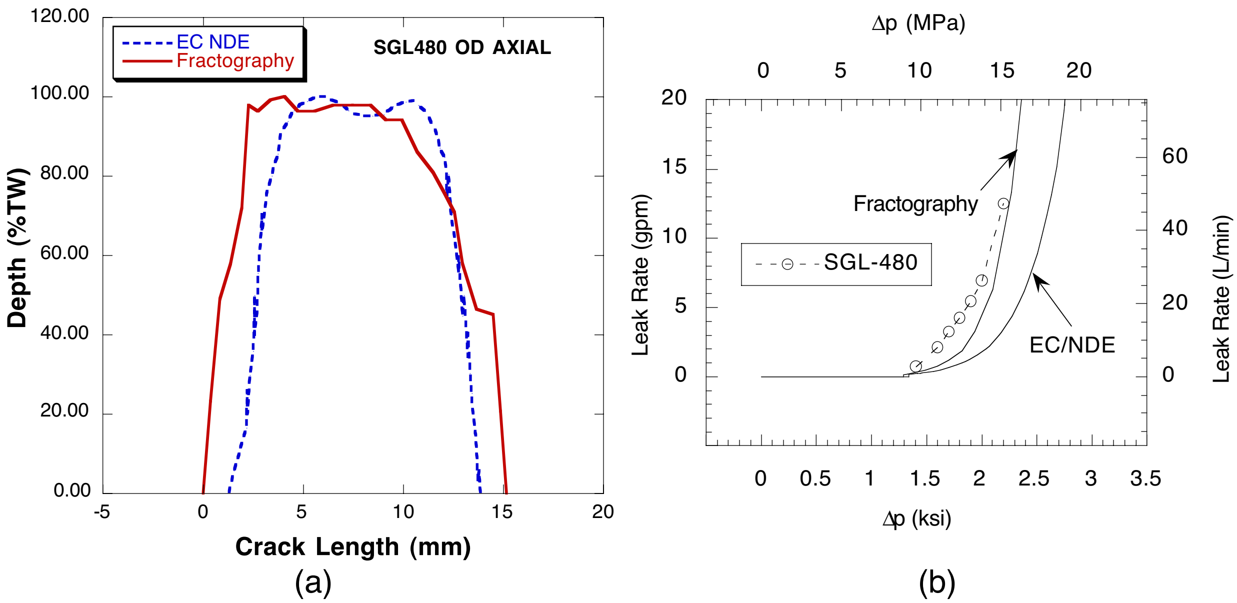

Fig. 3. (a) Crack depth profiles in specimen SGL 480 measured by pre-test EC and post-test fractography and (b) measured (symbols) and predicted (based on NDE and fractography depth data) pressure vs. leak rate plots for Test SGL-480. Room temperature.

Fig. 4. Post-test view of the OD surface of specimen SGL 480

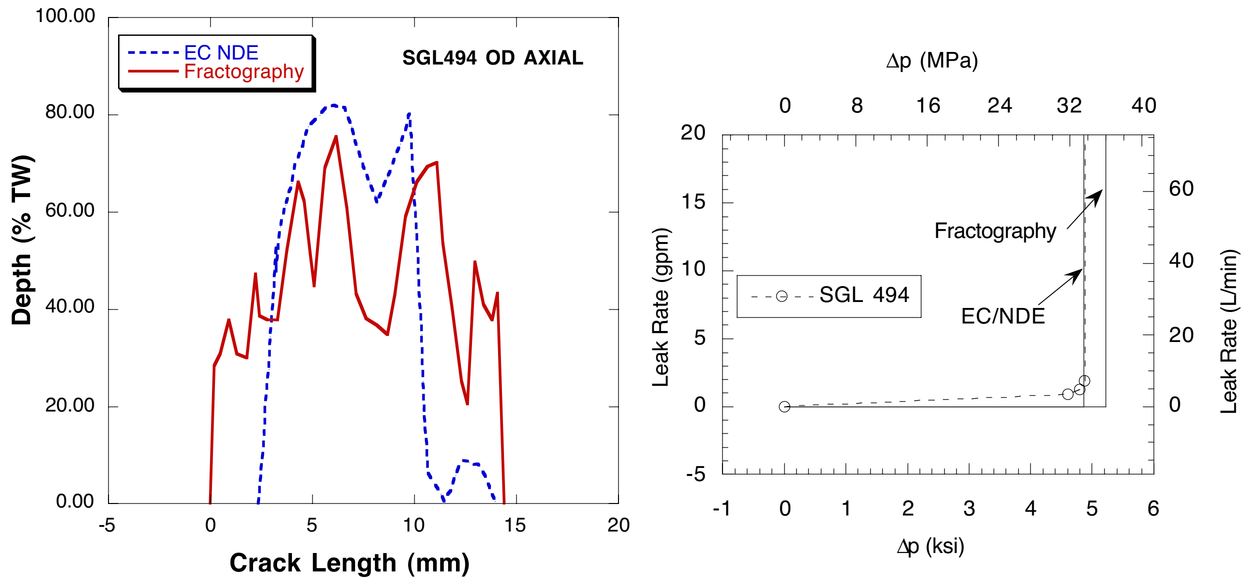

(a) (b)

Fig. 5. (a) Crack depth profiles in specimen SGL 494 measured by pre-test EC and post-test fractography and (b) measured (symbols) and predicted (based on NDE and fractography depth data) pressure vs. leak rate plots for Test SGL-494. Room temperature.

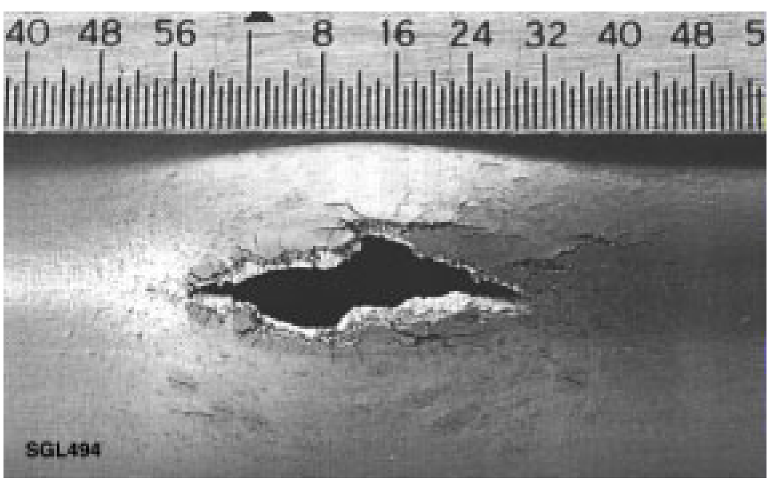

Fig. 6. Post-test view of the OD surface of specimen SGL 494.

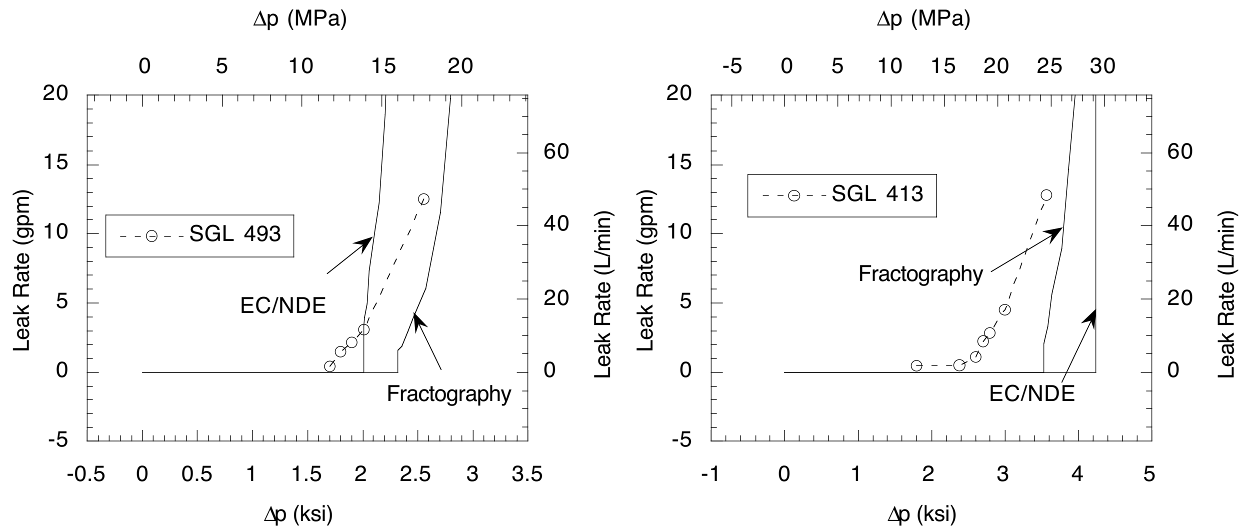

(a) (b)

Fig. 7. Measured and predicted (based on NDE and fractography depth data) pressure vs. leak rate plots for (a) test SGL-493 and (b) test SGL-413. Room temperature .

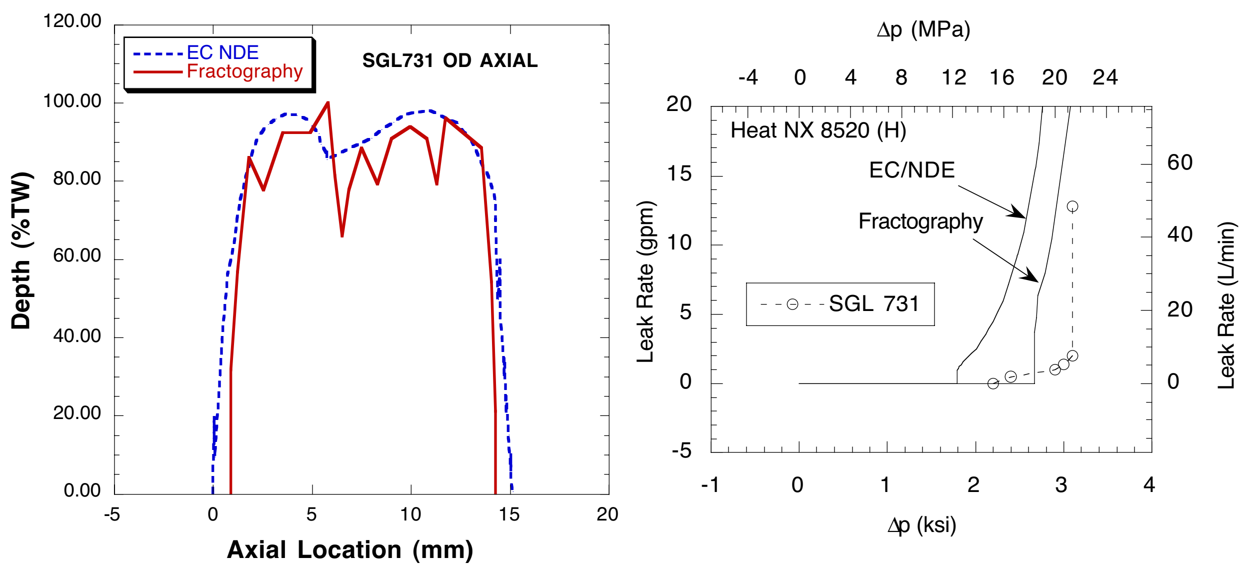

(a) (b)

Fig. 8. (a) Crack depth profiles by EC/NDE and fractography and (b) predicted and measured pressure vs. leak rate plots of test SGL-731. Room temperature.

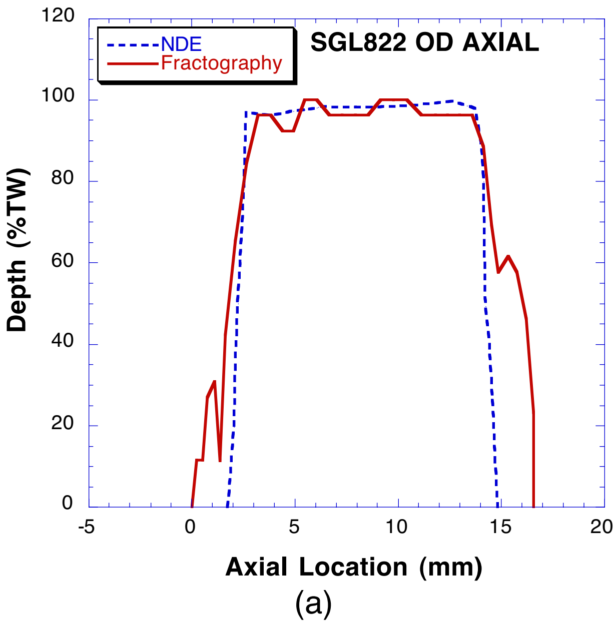

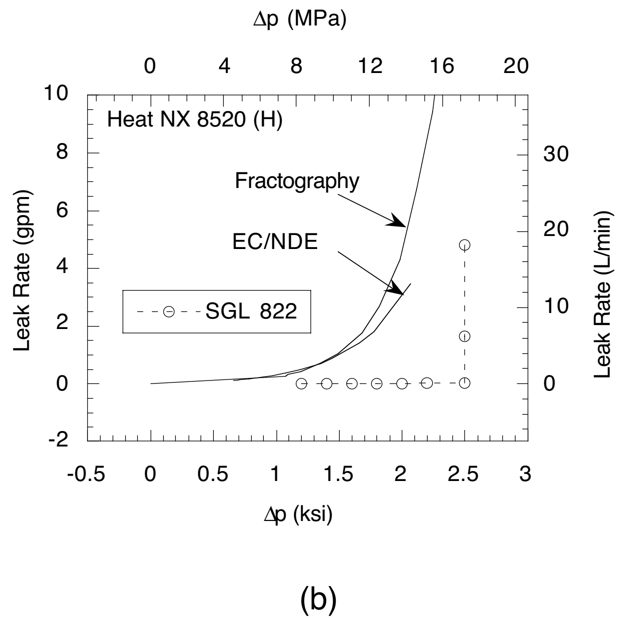

Fig. 9. (a) Crack depth profiles by EC/NDE and fractography and (b) predicted and measured pressure vs. leak rate plots of test SGL-822. Test temperature = 282°C.

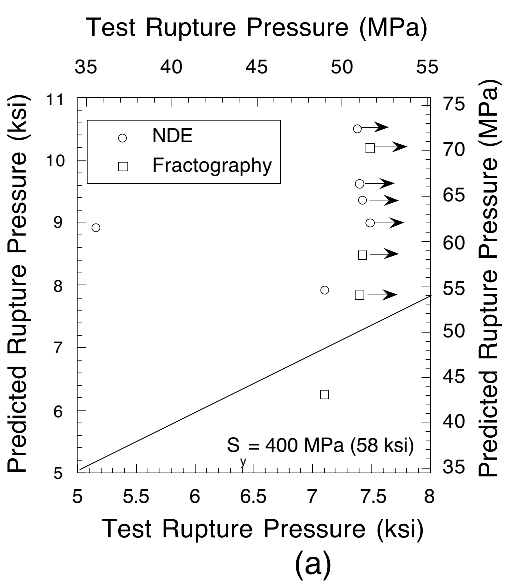

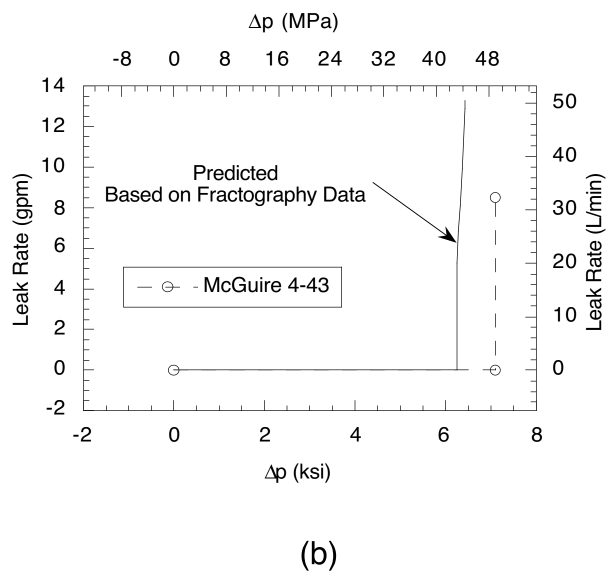

Fig. 10. (a) Observed vs. predicted rupture pressures for McGuire tubes (right arrows indicate no rupture) and (b) observed and predicted pressure vs. leak rats for McGuire test 4-43-2.